EasyChair Preprint

№ 6771

# FCM-DNN: Diagnosing Coronary Artery Disease by Deep Accuracy Fuzzy C-Means Clustering Model

Javad Hassannataj Joloudari, Hamid Saadatfar, Mohammad Ghasemigol, Roohallah Alizadehsani, Zahra Alizadeh Sani, Fereshteh Hasanzadeh, Edris Hassannataj and Danial Sharifrazi

EasyChair preprints are intended for rapid dissemination of research results and are integrated with the rest of EasyChair.

October 6, 2021

# FCM-DNN: Diagnosing Coronary Artery Disease by Deep Accuracy Fuzzy C-Means Clustering Model

**Javad Hassannataj Joloudari[1], Hamid Saadatfar[1], Mohammad GhasemiGol[1], Roohallah Alizadehsani[2], Zahra Alizadeh Sani[3,4], Fereshteh Hasanzadeh[4], Edris Hassannataj[5], Danial Sharifrazi[6]**

[1] Department of Computer Engineering, Faculty of Engineering, University of Birjand, Birjand, Iran
[2] Institute for Intelligent Systems Research and Innovation, Deakin University, Geelong, VIC 3216, Australia
[3] Rajaie Cardiovascular Medical and Research Center, Iran University of Medical Sciences, Tehran, Iran
[4] Omid hospital, Iran University of Medical Sciences, Tehran, Iran
[5] Department of Nursing, School of Nursing and Allied Medical Sciences, Maragheh Faculty of Medical Sciences, Maragheh, Iran;
[6] Department of Computer Engineering, School of Technical and Engineering, Shiraz Branch, Islamic Azad University, Shiraz, Iran

**Abstract:** Cardiovascular disease is one of the most challenging diseases in middle-aged and older people, which causes high mortality. Coronary Artery Disease (CAD) is known as a common cardiovascular disease. A standard clinical tool for diagnosing CAD is angiography. The main challenge is the dangerous side effects of this tool, which the situation of the disease can worsen. Today, the development of artificial intelligence-based decision-making methods is a valuable achievement for diagnosing clinical images. In this paper, artificial intelligence methods such as Neural Network (NN), Deep Neural Network (DNN), and Fuzzy C-Means clustering combined with Deep Neural Network (FCM-DNN) were developed for diagnosing CAD on Cardiac Magnetic Resonance Imaging (CMRI) dataset. To train the models, 10-fold cross-validation, 7-fold cross-validation, and 5-fold cross-validation techniques were used. As a result, the proposed FCM-DNN model has the best performance regarding the accuracy of 99.91% through the 10-FCV technique compared to the DNN and NN models reaching 99.63% and 92.18%, respectively, on the CMRI dataset. The results confirm that the proposed FCM-DNN method can be useful for CAD diagnosis in scientific and research centers.

**Keywords:** Coronary artery disease, Image analysis, Artificial intelligence, Neural network, Deep neural network, Fuzzy C-Means clustering

## 1. Introduction

Today, with the advent of new methods based on artificial intelligence, the diagnosis of diseases can be confirmed more quickly and accurately [1,2]. Researchers are trying to help develop computer-aided diagnosis systems i.e., computer vision/Machine Learning (ML), to diagnose the disease in the health care environment [1,3,4]. In recent years, the Deep Learning (DL) method has been an effective method for diagnosing medical images [5,6,7,8,9,10]. In this paper, Cardiac Magnetic Resonance Imaging (CMRI) dataset for Coronary Artery Disease (CAD) was used. Heart disease is an umbrella term that encompasses various diseases, including congenital diseases, CAD, and heart rheumatism. Based on the World Health Organization (WHO) report, CAD is the most common disease in middle-aged and older people, giving rise to killing more than 360,000 Americans in 2015 [11,12,13,14,15,16]. Moreover, according to the clinical centers for disease control and prevention statistics report, an American experiences a heart attack per 40 seconds [17].

Moreover, more than 75% of deaths had happened due to CAD in developing countries [11]. Regarding the mortality in men and women, more than 50% of the mortality has occurred caused by CAD to men, giving rise to 25% of deaths in the United States [18], and more than 630,000 Americans are dead per year [12], the cost of which has reached more than $ 200 billion [19].

In general, costs for heart patients will double by 2030, according to the American Heart Association [20]. Angiography is the most common tool for CAD diagnosis that has side effects for patients [17].

Hence, artificial intelligence-based methods have been proposed to replace angiography for CAD diagnosis. In this paper, artificial intelligence-based methods such as Neural Network (NN), Deep Neural Network (DNN), and Fuzzy C-Means combined with DNN were adopted. DNN was developed as an extended NN method, which leads to higher detection accuracy, lower false rate, and omit shift deviation [21]. In summary, the innovations of this paper are as follows:

- Providing CMRI dataset to diagnose the CAD for the first time
- using the combined FCM-DNN model to improve the automatic diagnosis of CAD based on CMRI analysis for the first time
- Improving the DNN training, avoiding over-fitting dataset applying FCM method before feeding images into DNN model, and also the Maxout selection and K-Fold Cross Validation (K-FCV) methods

In the current paper, the proposed FCM-DNN method has the best performance accuracy, precision, sensitivity, specificity, F1-score, False Positive Rate, False Negative Rate, and Area Under the Curve compared to the DNN and NN models.

As the latest scientific achievement, the FCM-DNN is performed for the first time using CMRI analysis.

Currently, to diagnose the severity of heart disease in patients, tools such as exercise stress testing, chest x-ray, computed tomography scan, CMRI, coronary angiography, and ECG are used [22,23]. In recent years, studies on the diagnosis of CAD have been run on ECG signals and numerical dataset using artificial intelligence methods.

In a study by Babaoglu et al. [24], CAD diagnosis was done using Genetic Algorithm (GA), Binary Particle Swarm Optimization (BPSO), and Support Vector Machine (SVM) based on exercise stress test data. In addition, GA and BPSO algorithms were created as feature selection techniques. In their study, 408 patients were tested through Exercise Stress Testing (EST) and coronary angiography.

A total of 23 features were extracted from the EST dataset. Using the BPSO algorithm, the diagnosis accuracy rate reaching 81.46% is the best compared to the GA and SVM algorithms achieving 79.17% and 76.67%, respectively.

Kumar et al. [25] have used ECG signals including 40 healthy subjects and seven subjects for CAD diagnosis. These signals were mapped into pulses, which were decomposed mainly by analytical wavelet transform. For classification, Least Squares Support Vector Machine with the Radial Basis Function (RBF) kernel was used. As a result, more accuracy was obtained as 99.60% for the Violet kernel or Morlet wavelet kernel compared to the RBF kernel reaching 99.56% through the 10-Fold Cross-Validation (10-FCV) technique.

Alizadehsani et al. for CAD diagnosis, the classification methods such as Sequential Minimal Optimization (SMO) and Naïve Bayes (NB) both separately and in combination based on ECG symptoms and characteristics on 303 samples have suggested [26]. The 10-FCV technique was used to evaluate the algorithms. As a result, using the SMO-NB algorithm, they have achieved greater accuracy of 88.52% than the SMO and NB algorithms of 86.95% and 87.52%, respectively.

In another study, Alizadehsani et al. [27] have proposed classification algorithms such as SMO, NB, bagging with SMO, and neural network for CAD diagnosis on 303 numerical data with 54 features. To determine the essential features, the Information Gain (IG) and confidence methods were used. Among the algorithms, the SMO algorithm with IG has the best performance regarding accuracy rate of 94.08% through the 10-FCV technique was.

Alizadehsani et al. have presented C4.5 decision tree and bagging algorithms on 303 numerical dataset to diagnose CAD disease [28]. They have used IG and Gini Index (GI) methods for feature selection. In the CAD diagnosis test, coronary artery stenosis was examined, including Left Anterior Descending (LAD), Left Circumflex (LCX) (LCX; for the left coronary artery), and Right Coronary Artery (RCA). In addition, the accuracy of the algorithms was computed based on the 10-FCV technique. As a result, the bagging algorithm with feature selection method and GI has better performance than the C4.5 decision tree. The accuracy of the bagging algorithm for diagnosing three coronary artery stenosis, including LAD, LCX, and RCA, was 79.54%, 65.09%, and 66.31%, respectively. However, the accuracy of diagnosis using the C4.5 decision tree was obtained as 76.56%, 63.10%, and 63.38% for stenosis of LAD, LCX, and RCA, respectively.

Alizadehsani et al. have applied the SVM method on 303 patients with 54 features to diagnose CAD. Through demographic, symptom and examination, ECG, laboratory, and echo characteristics, stenosis of the three large coronary arteries was diagnosed separately [29]. They also have used analytical methods to explore the significance of vascular stenosis features. Using the SVM method with feature selection methods such as combined information gain and average information gain, accuracy rates of 86.14%, 83.17%, and 83.50% for the diagnosis of the stenosis of LAD, LCX and RCA were obtained, respectively.

Dolatabadi et al. [30] have studied the combined method of Principal Component Analysis (PCA) and optimized SVM to diagnose CAD on Heart Rate Variability (HRV) signal extracted from the ECG. The PCA method was used to reduce the dimensions of the features and computational complexity. Furthermore, the optimized SVM method refers to the optimization of cost and sigma parameters. Therefore, the diagnostic accuracy obtained through the combined method was 99.2%, and accuracy was achieved by 90.62% using the standard SVM method.

Arabasadi et al. have examined neural network and genetic algorithms for CAD diagnosis on 303 numerical samples [31]. For feature selection, feature ranking methods such as weight by SVM, GI,

IG, and PCA were specified. As a result, using the neural network algorithm and the combined neural network-genetic algorithm, the accuracy rates of 84.62% and 93.85% were obtained, respectively.

Alizadehsani et al. [32] have utilized a feature engineering method for improving CAD diagnosis on the 500 samples. This method exploits the results related to the NB, C4.5, and SVM classifiers for the non-invasive diagnosis of CAD disease. They also have performed the weight by SVM method as a feature selection method. Based on the NB, C4.5, and SVM classifiers, accuracy rates of 86%, 89.8%, and 96.40% were achieved, respectively.

In a study by Abdar et al. [33], a hybrid two-level genetic algorithm and nuSVM namely, the N2Genetic-NuSVM method, were conducted for CAD diagnosis on 303 samples. They have used a two-level genetic algorithm to optimize the SVM parameters, and they have also accomplished feature selection applying the GA algorithm. By using the proposed method, an accuracy of 93.08% was achieved.

In other studies conducted by Miaoa and Miaoa [34], a DNN model has been presented for CAD diagnosis on the Cleveland Clinic Foundation dataset with 303 patients. The proposed DL model includes 28 input units, first and second hidden layers, and a binary output unit, in which 105 neurons in the first layer and 42 neurons in the second layer are considered, and 50% dropout is assigned. The output unit is connected to a sigmoid activation function in the final stage. An accuracy of 83.67% using the proposed method was obtained.

Hamersvelt et al. have examined a Convolutional Neural Network (CNN) to diagnose CAD on the coronary artery angiography CT images at rest with 126 patients [35]. As a result, by applying the proposed CNN method, an accuracy of 71.1% was achieved.

Hassannataj et al. [17] have extracted essential features of the CAD, which was diagnosed using the random trees (RTs) on the 303 samples with 55 features. They have compared the RTs model with SVM, the C5.0 decision tree, and the CHAID decision tree classification models. As a result, using the RTs model, 40 features were extracted with an accuracy of 91.47%, which RTs model has the best performance compared to the other models.

Acharya et al. [36] have implemented the CNN method for CAD diagnosis applying different periods of ECG signal segments from the PhysioNet database [37]. In their study, an 11-layer CNN structure, including four convolutional layers, four max-pooling layers, and three fully-connected layers for 2 seconds in the first network with 95300 sections and five seconds with 38,120 sections in the second network was developed. The proposed CNN model led to the accuracy of 94.95% for the first network and 95.11% accuracy for the second network.

Tan et al. [38] have introduced a long-term short-term memory (LSTM) neural network model combined with CNN for CAD diagnosis based on ECG signals from the PhysioNet database. Accordingly, an 8-layer stacked convolutional LSTM network has been determined in their research. This 8-layer model consists of layers 1 to 4 related to 2 convolutional layers and two layers of max pooling for the CNN structure, and layers 5 to 7 are associated with LSTM layers. The last layer is a fully connected layer as the classification layer. They have achieved an accuracy of 99.85%.

Acharia et al. [39] have investigated the K-Nearest Neighbor (KNN) classifier to classify and diagnose CAD on ECG signals. For feature extraction, they have used methods such as discrete cosine transform, discrete wavelet transform, and empirical signal decomposition mapped into intrinsic state components. Besides, these methods were compared to one another in the disease diagnosis process. ECG signals were also applied to the appropriate transformation methods to obtain coefficients. Then the features were reduced using the locality preserving projection method, and the reduced features

were ranked applying the analysis of variance technique. In the following, high-ranking features were fed to the KNN classifier. As a result, the proposed model on only seven features through the discrete cosine transform method had the best performance regarding the accuracy of 98.5%.

Acharya et al. [40] have presented CNN method to diagnose CAD on ECG signals. The dataset includes 30,000 patients and 110,000 healthy. As a result, using the proposed method, they have obtained 98.97% accuracy by applying the 10-FCV technique.

In a study by Ghiasi et al. [41], a regression and classification tree model under the CART model on the Z-Alizadehsani dataset [27] with 303 patients and 55 features to diagnose CAD have been investigated. They compared their model with classification models such as SMO, bagging, bagging with SMO, NB, artificial neural network, J48 decision tree, and C4.5. The accuracy rate of 100% using the CART model for CAD diagnosis was gained.

To identify risk factors for CAD, Verma et al. [42] have performed a combined model of Correlation-based Feature Subset (CFS) selection with Particle Swarm Optimization (PSO) and K-Means clustering algorithm on 335 samples of the 26 features. After applying CFS and PSO, five features were identified as risk factors. In addition, Multi-layer Perceptron (MLP), Multinomial Logistic Regression (MLR), fuzzy unordered rule induction algorithm, and C4.5 decision tree were implemented for CAD diagnosis. As a result, more accuracy of 88.4% using the MLR algorithm was obtained.

Idris et al. [43] have developed data mining models to predict the CAD, including NN, Logistic Regression (LR), KNN, NB, SVM, deep learning, and Vote (an ensemble method with NB and LR) on National Cardiovascular Disease-Acute Coronary Syndrome (NCVD-ACS) from the University Malaya Medical Centre (UMMC) and Sultanah Aminah Hospital (SAH) data sets in Malaysia. Feature selection methods such as the Chi-squared test, recursive feature elimination, and the embedded decision tree were applied. The prediction accuracy rate of 94.5% was gained through the NN method combined with the embedded decision tree method on the UMMC dataset. Moreover, using the same method, an accuracy rate of 89.7% was obtained on the SAH dataset.

Velusamy and Ramasamy [44] have examined three classification methods, including SVM, random forest, and KNN, for CAD diagnosis on the Z-alizadehsani. The results of these classifiers were combined based on weighted-average voting, majority-voting, and average-voting methods. According to the weighted-average voting method and five selected features, the accuracy rate of 98.97% has a better performance than other classifiers on the original Z-alizadehsani dataset. Also, the accuracy for the proposed algorithm on the Z-alizadehsani balanced dataset was obtained as 100%.

According to the latest scientific achievements in the field of CAD diagnosis, we used the FCM-DNN method on the CMRI dataset for the first time.

The rest of this paper is structured as follows:

The proposed methodology is presented in Section 2. Evaluation of models, results, and findings of research regarding the experiments are expressed in section 3, and finally, in section 4, the conclusion and future works are described.

## 2. Methodology

In this paper, for classifying and diagnosing CAD, NN, DNN, and Fuzzy C-Means clustering combined with Deep Neural Network (FCM-DNN) methods were used on the CMRI dataset.

Hence, the proposed methodology has been conducted in 6 different phases. These phases include

collecting clinical image sets related to CMRI dataset for both healthy and sick subjects, data preprocessing, CMRI dataset partitioning, classification models, evaluation criteria of models, results, and interpretation of experiments according to the CMRI dataset classification and diagnosis of the CAD.

The proposed methodology is shown in Figure 1. In the following, the phases of the proposed methodology are described in detail.

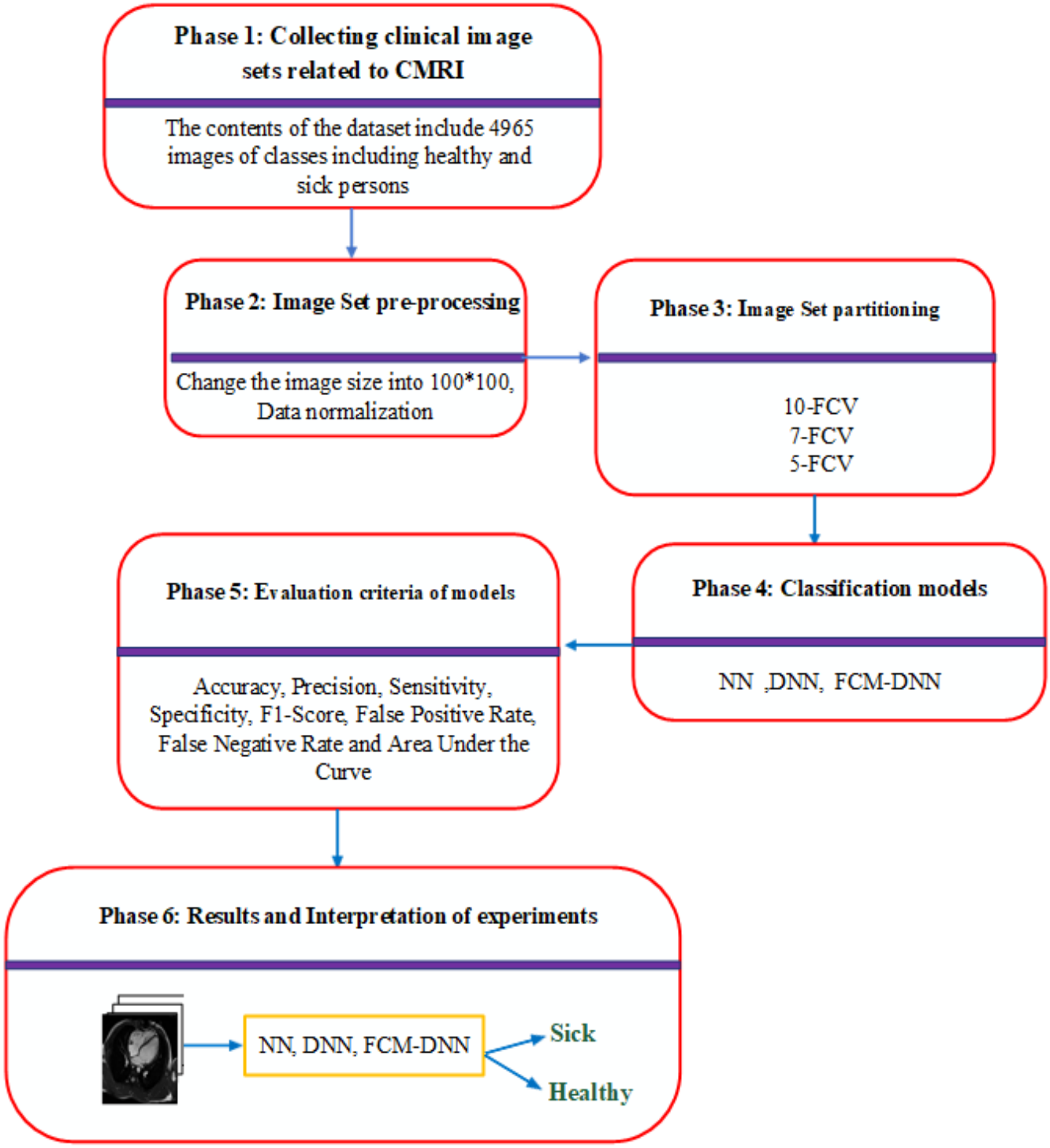


**Figure 1.** The proposed methodology.

*Phase 1: Collecting clinical CMRI dataset*

The first phase was the extraction of CAD clinical image sets related to CMRI, which this dataset was provided from Milad Hospital in Tehran, IRAN, by Z. Alizadehsani. In this paper, the used dataset includes 4965 images, so that 2569 images of healthy on 16 subjects and 2396 images of sick on 14subjects. All images are on a Grayscale level.

Also, the dimensions of images related to both healthy and sick subjects are various. For example, four images of healthy and sick subjects are illustrated in Figures 2 and 3, respectively.

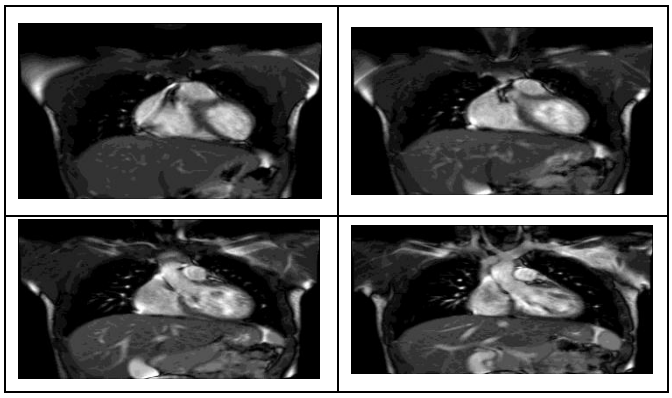

**Figure 2.** The images of healthy subjects.

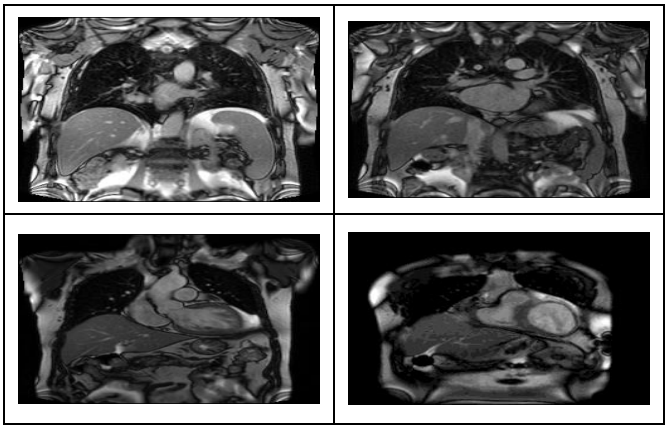

**Figure 3.** The images of sick subjects.

In addition, the statistical characteristics of our dataset for healthy and sick subjects are stated in Tables 1 and 2, respectively.

**Table 1.** The statistical characteristics of the CMRI dataset for healthy subjects.

| Statistics | Age | Weight | Height |
|---|---|---|---|
| Mean | 34.75 | 65.13 | 165.75 |
| Std. Error of Mean | 4.955 | 4.531 | 3.322 |
| Median | 34.50 | 69.50 | 170.00 |
| Std. Deviation | 19.821 | 18.125 | 13.289 |

| | | | |
|---|---|---|---|
| Variance | 392.867 | 328.517 | 176.600 |

Table 2. The statistical characteristics of the CMRI dataset for sick subjects.

| Statistics | Age | Weight | Height |
|---|---|---|---|
| Mean | 59.86 | 70.79 | 170.71 |
| Std. Error of Mean | 3.797 | 2.881 | 2.286 |
| Median | 64.50 | 72.00 | 169.50 |
| Std. Deviation | 14.206 | 10.779 | 8.552 |
| Variance | 201.824 | 116.181 | 73.143 |

*Phase 2: Data preprocessing*

In the samples analysis process, preprocessing is required on the samples. Images of healthy and sick persons were different in size, which changed into a 100*100 dimension.

Furthermore, one of the available approaches for preprocessing on image samples, data normalization, is between 0 and 1. The normalization increases the accuracy of clustering and the accuracy of classification models, and also it reduces the false rate for clustering. The type of normalization method, interval transformation, was determined, i.e., the sample set was normalized between 0 and 1.

Indeed, by normalizing the images, the light intensity of the images becomes to intervals 0 and 1.

*Phase 3: Image Set partitioning*

For the partitioning Phase of the CMRI dataset, the K-FCV technique was used, and the data were divided based on the 10-FCV, 7-FCV, and 5-FCV. Based on the K-FCV technique, the images are divided into K parts, so that K-1 parts are used for training and 1 part for testing. By rotating the test image set, the K-FCV process is repeated K times.

As a result, using the K-FCV technique leads to having more data as training data points to develop the expected model. In addition, the K-FCV technique was used for avoiding over-fitting of the data, for improving the generalization, and for reducing the training loss.

For this purpose, using 10-FCV, nine-tenths of the data for the training and one-tenth of the remaining data for testing is applied in each fold. Again, on nine-tenths of training of the data, eight-tenths for training and two-tenths for validation were executed at ten times.

Also, using 7-FCV, six-sevenths of the data are applied for training and one-seventh of the remaining data for testing in each fold. Once again, based on the six-seventh training of the data, eight-tenths for training and two-tenths for validation of the model were conducted at seven times.

Using 5-FCV, four-fifths of the data are examined to each fold for the training of the data, and one-fifth of the remaining data are applied for testing. Then eight-tenths of the data for training and two-tenths for validation on one-half of training of the data at five times was accomplished. The partitioning process for training, testing, and validation of the CMRI dataset through 10-FCV, 7-FCV, and 5-FCV is shown in Figures 4, 5, and 6, respectively.

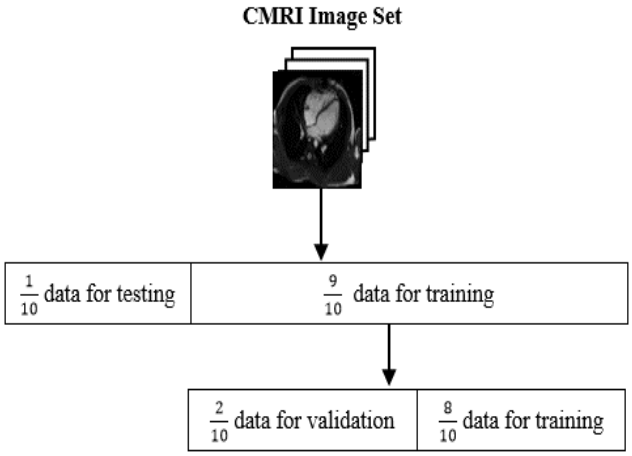


**Figure 4.** The partitioning process using the 10-FCV technique.

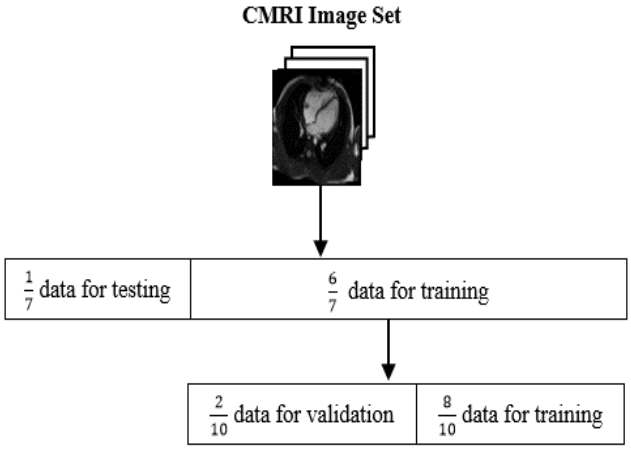


**Figure 5.** The partitioning process using the 7-FCV technique.

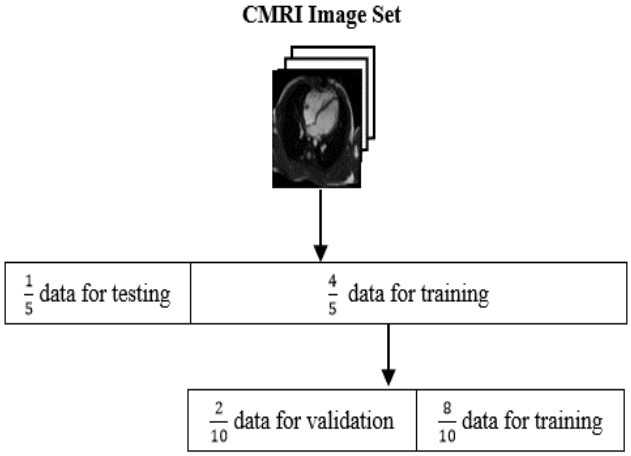


**Figure 6.** The partitioning process using the 5-FCV technique.

*Phase 4: Classification models*

In this paper, the developed classification models are NN, DNN, and FCM-DNN. The creation of the models is described in detail.

1) Creating NN model

In this paper, the created NN model is a 4-layer model. The first layer is related to the input images of the NN model.

The second and third layers were specified as the hidden layers with three neurons. The learning rate is 0.3. Also, the momentum value is assigned as 0.2. The NN model is shown in Figure 7.

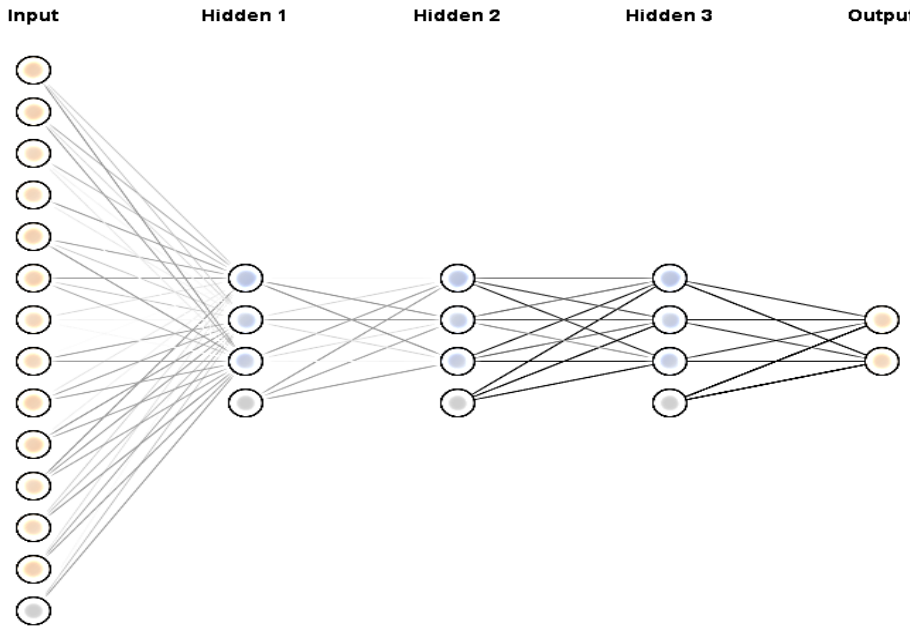


**Figure 7.** The NN model.

2) Creating DNN model

The DNN model was created with the size of the hidden layers as 50*50 at 50 epochs. The model is an 8-layer model including one input layer of the images, six hidden layers, and one output layer. Maxout [45,46] is determined as the nonlinear activation function, which assigns the activity of neurons in the hidden layers of the network.

Indeed, the Maxout selects the utmost coordinate of the network input vector, which is effective for over-fitting of the input data and improving the deep network training. The DNN model is demonstrated in Figure 8.

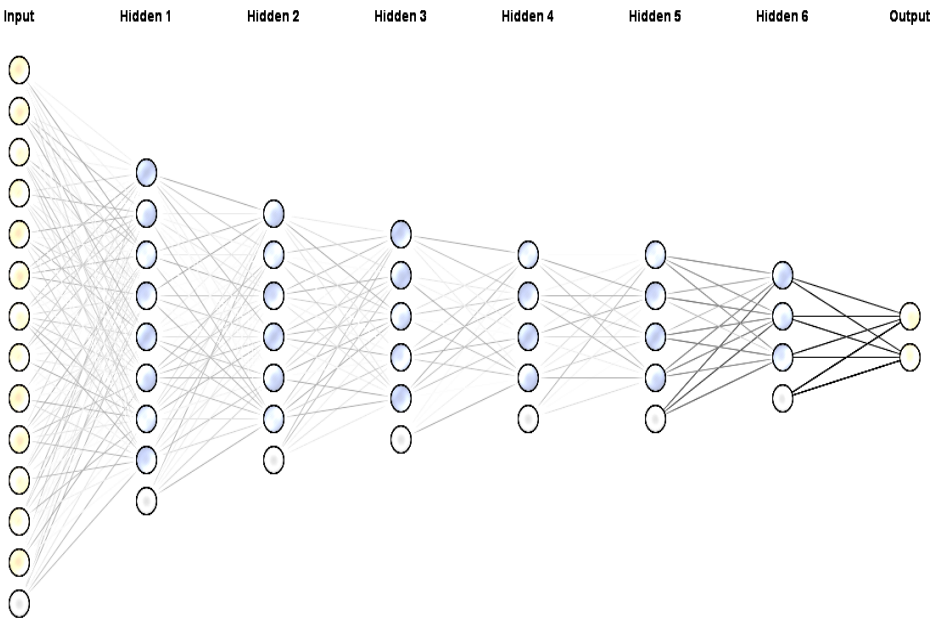


**Figure 8.** The DNN model.

To classify healthy subjects from sick subjects to the range of 0 (number 0, i.e. the subject is sick) and 1 (number 1, i.e. the subject is healthy), the sigmoid function [47,48] is assigned in the last layer. Also, the Cross-Entropy (CE) function [49] is determined as the loss function. The formulas for these functions are defined as follows.

$$F(S_i)=\frac{1}{1+e^{-S_i}} \quad , S= \quad Fx_i \quad , w \qquad (1)$$

$$CE(S.y) = -\sum_{i=1}^{C} y_i \log\left(F(S_i)\right) \qquad (2)$$

According to (1), the output value for the decision boundary ($Si$) or the probability value of the predicted class is 0 or 1, ($x_i$) is the input image, and $w$ is the weight. Also, based on (2), $C$ represents the number of classes, and $y_i$ indicates the predicted value for the desired class. Since, in this paper, the number of classes is 2, the $CE$ function is calculated as follows.

$$CE(S.y) = -\sum_{i=1}^{C} y_i \log\left(F(S_i)\right) = -y_1 \log\left(F(S_1)\right) - (1-y_1)\log(1-F(S_1)) \qquad (3)$$

According to (3), $F(S_2)$ is equal to $1\text{-}F(S_1)$.

3) Creating FCM-DNN model

Clustering is a common descriptive method identifying a finite set of categories/clusters for describing similar data. In other words, clustering is the grouping of samples with similar characteristics that the samples in one group have the most similarity to each other and the most difference from the samples in other groups. Each cluster has a center that the degree of similarity of the data to the center of the cluster is generally determined by a parameter called the similarity criterion /distance criterion [50]. Indeed, in clustering, the similarity criterion is determined based on maximizing separation between clusters.

Therefore, in clustering, the categories are not predefined, and the data grouping operation is done without supervising or without labeling, i.e. the training data do not have a label. The suitable performance of a clustering method is such that the samples in different clusters have the least similarity to each other.

The common clustering model is shown in Figure 9.

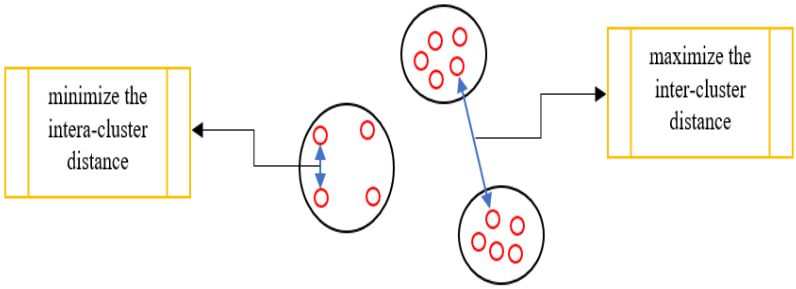


**Figure 9.** The concept of clustering.

In general, the goal in all clustering methods is to minimize the intera-cluster distance and maximize the inter-cluster distance [51].

Common clustering algorithms in vector quantification are K-Means [52,53], K-Medoids [54], and FCM. Since FCM clustering is used in this paper, this method is described in detail below.

The FCM method was first proposed in 1973 by Duda and Hart [55], which performs a more accurate clustering than classic clustering under uncertainty conditions such as K-Means and K-Medoids.

In the current paper, since the images were attached to different clusters, the classic clustering methods were not suitable in that the images should be placed in more than one cluster. To solve the problem of placing the images in more than one cluster, a fuzzy version of the C-Means method was proposed by Don [56]. Next, the FCM method was developed by Bezdek [57], in which a fuzzy factor of *m* as fuzzifier was created.

In FCM clustering, unlike classical clustering, each sample can belong to two clusters and more than two clusters. The main idea of the FCM clustering is that a sample can belong to more than one cluster with a membership degree between 0 and 1 based on the membership function/objective function [58,59,60,61].

In the FCM method, the membership function is as follows:

$$\min j_m(u.v) = \sum_{i=1}^{c}\sum_{k=1}^{n} u_{ik}{}^m d_{ik}{}^2 = \sum_{i=1}^{c}\sum_{k=1}^{n} u_{ik}{}^m \left\|x_k - v_i\right\|^2 \quad (4)$$

In (4), the variable *m* is a real number more than 1, which in most cases is assigned to 2 for the variable *m*. In the given formula, if the variable *m* is set equal to 1, the objective function for C-Means clustering is obtained. Also, in the stated formula, the variable $X_k$ is the sample *K*, $V_i$ is the center of the cluster, the number of clusters "*C*" is predetermined, and *n* represents the number of samples. $U_{ik}$ indicates the degree of belonging of sample *i* to the cluster *k*. $d_{ik} = \left\|x_k - v_i\right\|$ is the distance between the sample $X_k$ from the cluster center $V_i$. The most crucial similarity criteria for solving clustering problems is the distance criterion "*j*", which should be minimized. In other words, the FCM method determines

the data for each cluster based on the distance between the cluster center and the data points by assigning membership to each data based on the membership function.

In summary, the FCM method includes the following steps.

- *C* cluster centers are randomly assigned.
- The distance of each sample to the center of the cluster is obtained.

$$U_{imi} = \frac{\frac{1}{d_{imi}}}{\frac{1}{d_{imi}} + \frac{1}{d_{imj}}} \quad (5)$$

According to *(5)*, *d* represents the distance between each sample to the cluster centers $m_i$ and $m_j$, and $U_{imi}$ indicates the degree of belonging to each sample.

- New centers of clusters are obtained using fuzzy means. If we have two clusters, the new centers of the clusters are achieved as follows.

$$m_1 = \frac{\sum_{i=1}^{N} X_i U_{i1}}{\sum_{i=1}^{N} U_{i1}}, m_2 = \frac{\sum_{i=1}^{N} X_i U_{i2}}{\sum_{i=1}^{N} U_{i2}} \quad (6)$$

According to (*6*), $X_i$ represents the sample *i*, and $m_1$ and $m_2$ are the cluster centers.

- Finally, fuzzy intra-cluster-based the sum of the distances under membership function "*J*" is calculated, which must be optimized.

$$J = \sum_{j=1}^{C} \sum_{i=1}^{N} U_{ij} d_{ij} \quad (7)$$

Based on (*7*), *J* is the sum of the distances, "*C"* is the number of clusters, "*Uij"* is the degree of belonging of sample *i* to the cluster *j*, and *"*$d_{ij}$*"* is the distance of sample *i* to the center *j*. For two consecutive iterations, if the sum of distance is less than the threshold value, the FCM method terminates. In this situation, new cluster centers are determined again.

Therefore, the advantage of the proposed FCM method is that this method is always convergent and always has a rapid convergence in reaching the final solution, i.e., the FCM method converges to a local optimum.

Despite the good advantages of the FCM method, the disadvantage of this method compared to the classic clustering method is more computational time. The reason for this problem is the additional calculations for determining each data to all clusters. But the crucial advantage of clustering data using the FCM method is to achieve higher accuracy.

In this paper, the FCM-DNN method was examined on the CMRI dataset. Firstly, the dataset was clustered for identifying the clusters by the FCM method. The number of the cluster was assigned as 10. It should be noted that the images were initially labeled as healthy and sick subjects. The labels have been removed for clustering. Then for clustering operations, 10 clusters were determined, that 5 clusters are for healthy subjects and 5 clusters are for sick subjects.

After applying fuzzy clustering, the generated dataset is fed to the DNN model for classifying the CMRI dataset. The developed FCM-DNN model diagnoses the input image between 10 clusters, including healthy and sick classes.

## 3. Experimental Results and Discussion

Due to the fifth phase of the proposed methodology, using a Confusion Matrix (CM), the evaluation criteria for the models, including accuracy (ACC), precision or Positive Predicted Value (PPV), sensitivity (SEN), specificity (SPC), F1-score, False Positive Rate (FPR), False Negative Rate (FNR), and Area Under the Curve (AUC) were measured [62]. The CM includes True Positive (TP), False Positive (FP), True Negative (TN), and False Negative (FN) elements. The CM is described for this paper in Table 3.

**Table 3.** The CM for this paper.

| Actual class | The predicted class | |
|---|---|---|
| | Sick(Positive) | Healthy(Negative) |
| Positive | TP | FP |
| Negative | FN | TN |

According to Table 3, the elements of the CM are defined as follows:

TP: The number of positive samples that have been correctly diagnosed patients by testing.

FP: The number of positive samples that have been wrongly diagnosed healthy by testing.

TN: The number of negative samples that have been correctly diagnosed healthy by testing.

FN: The number of negative samples that have been wrongly diagnosed patients by testing.

Indeed, the CM is a valuable tool for analyzing how the classification models perform for diagnosing data in different categories. If the data are in the $M$ category, a classification matrix is a table with a minimum size of $M*M$. Ideally, most of the data should be on the original diameter of the matrix, i.e., the values for the TP and TN elements and the rest of the matrix values should be zero or close to zero [63].

The formulas for the evaluation criteria for the models are given below.

$$ACC = \frac{TP+TN}{FP+FN+TP+TN} \quad (8)$$

$$PPV = \frac{TP}{TP+FP} \quad (9)$$

$$SPC = \frac{TN}{TN+FP} \quad (10)$$

$$SEN = \frac{TP}{TP+FN} \quad (11)$$

$$F1-Score = \frac{2TP}{2TP+FP+FN} \quad (12)$$

$$FPR = 1 - SPC \quad (13)$$

$$FPR = 1 - SEN \quad (14)$$

It should be noted that the FPR criterion is more important than the FNR for clinical centers in identifying more risks [63,64].

The results regarding the evaluation criteria for the models are illustrated based on the number of folds in Table 4. Implementation of models has been done using RapidMiner software version 9.5.01 [46].

According to Table 4, the ACC, PPV, SEN, SPC, F1-score, FPR, FNR, and AUC rates using NN, DNN, and FCM-DNN methods on the CMRI dataset were obtained.

The most crucial criterion for diseases diagnosis is ACC that the ACC rate for CAD diagnosis using the proposed FCM-DNN is more than NN and DNN methods.

The ACC of the FCM-DNN method through the 10-FCV technique was obtained as 99.91% on 4965 images, while the accuracy of DNN and NN methods was obtained as 99.63% and 92.18%, respectively.

In addition, the FPR and FNR criteria are essential for determining the false rate for diagnosing the disease for clinical centers, because the FPR is more valuable than FNR for identifying more risks. The FPR value using the proposed FCM-DNN method was achieved as zero, and the FNR value was gained as 0.18.

Also, the value of the FPR using the DNN method was gained as 0.42, and the FNR value was obtained as 0.32. Moreover, the FPR value using the NN method was calculated as 12.21, and the FNR value was obtained as 3.56. As a result, the FCM-DNN method has a lower false rate than the NN and DNN classification methods.

As a significant result, there is a crucial criterion for evaluating the classification models, namely AUC, which indicates the accuracy of the level below the Receiver Operating Characteristic (ROC) curve.

Based on the 5-FCV, 7-FCV and 10-FCV techniques, the ROC diagram for the NN, DNN and FCM-DNN models are shown in Figures 10 ((a), (b)), 11 ((a), b)) and 12, respectively.

According to figure 10 (a), the AUC value for the NN method through the 5-FCV and 10-FCV techniques was obtained as 93.3%.

Also, based on Figure 10 (b), the AUC value for the NN method through the 7-FCV technique was achieved as 93.6%.

[1]https://docs.rapidminer.com/latest/studio/operators/modeling/predictive/neural_nets/deep_learning.html

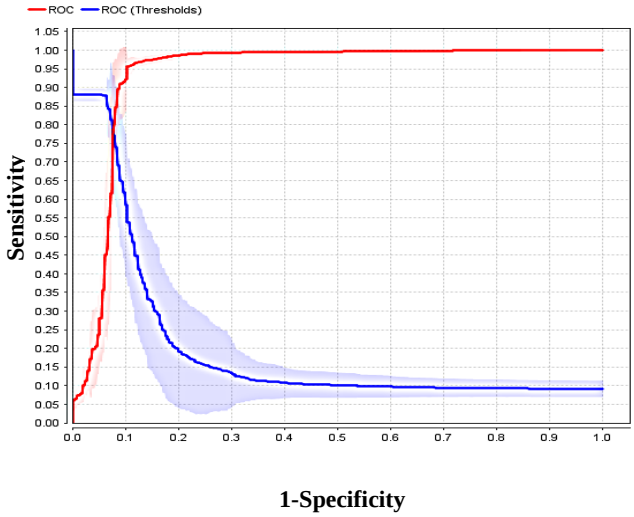


**Figure 10 (a).** The AUC diagram for the NN method through the 5-FCV and 10-FCV techniques.

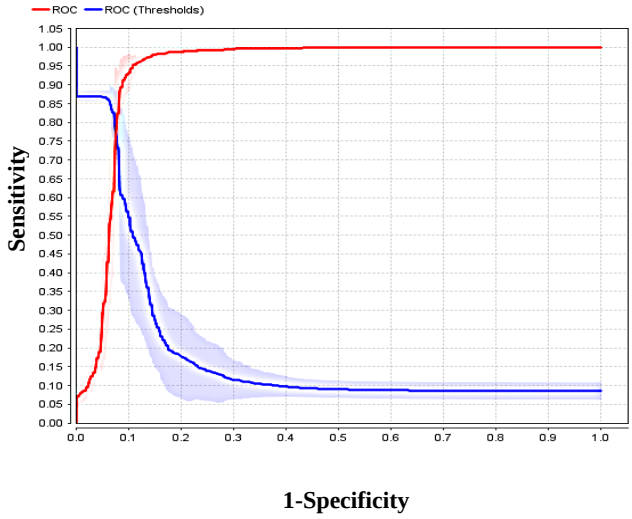


**Figure 10 (b).** The AUC diagram for the NN method through the 7-FCV technique.

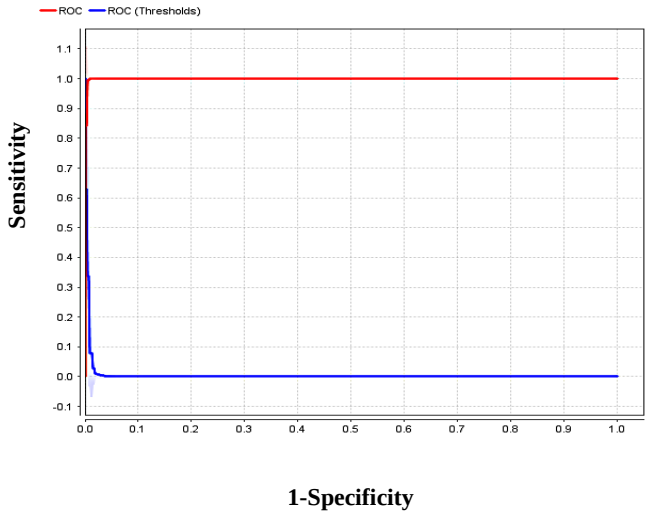


**Figure 11 (a).** The AUC diagram for the DNN method through the 10-FCV and 5-FCV techniques.

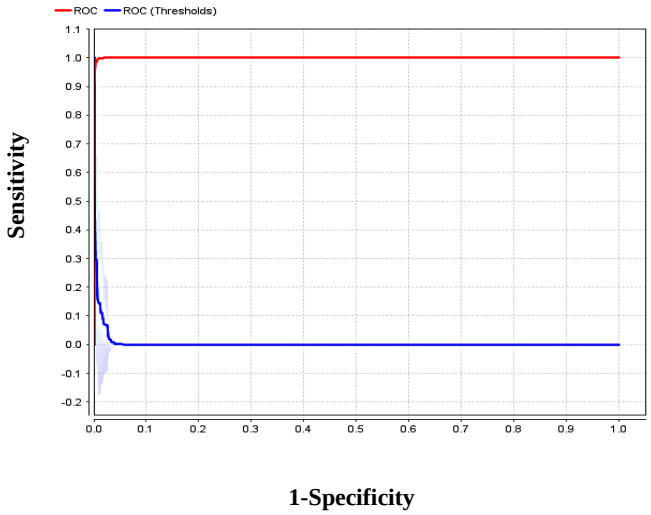


**Figure 11 (b).** The AUC diagram for the DNN method through the 7-FCV technique.

The AUC value for the DNN method based on the 10-FCV and 5-FCV techniques was gained as 99.9% related to figure 11 (a).

The AUC value for the DNN method based on the 7-FCV technique was computed 100% of Figure 11(b).

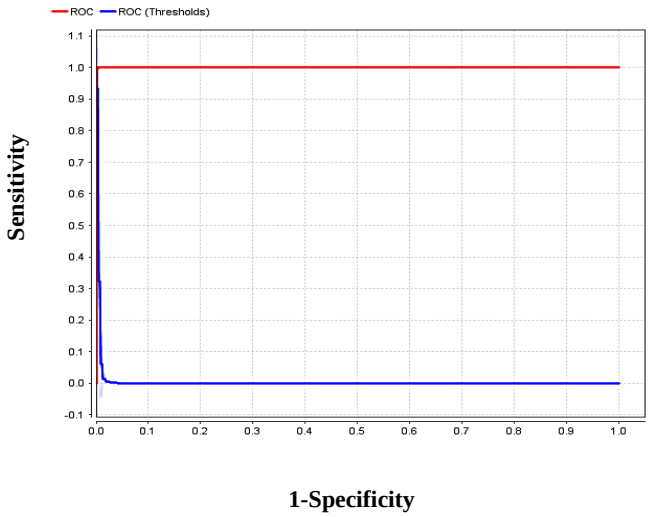


**Figure 12.** The AUC diagram for the FCM-DNN method through the 10-FCV, 7-FCV, and 5-FCV techniques.

Based on Figure 12, the AUC value for the FCM-DNN method through the 10-FCV, 7-FCV, and 5-FCV techniques was obtained as 100%.

As a result, the FCM-DNN model has the best AUC compared to the NN and DNN models based on the 10-FCV, 7-FCV, and 5-FCV techniques.

In the following, the performance of the proposed models has been compared based on the different criteria, which is depicted in Figure 13.

**Table 4.** Results of models evaluation criteria on the CMRI dataset.

| The methods | Number of Folds | ACC (%) | PPV (%) | SEN (%) | SPC (%) | F1-Score (%) | FPR | FNR | AUC (%) |
|---|---|---|---|---|---|---|---|---|---|
| NN | 5 | 92.18 | 89.28 | 96.44 | 87.79 | 92.66 | 12.21 | 3.56 | 93.3 |
| | 7 | 91.79 | 89.89 | 94.57 | 88.93 | 92.07 | 11.07 | 5.43 | 93.6 |
| | 10 | 92.18 | 89.28 | 96.44 | 87.79 | 92.66 | 12.21 | 3.56 | 93.3 |
| DNN | 5 | 99.35 | 99.19 | 99.54 | 99.15 | 99.36 | 0.85 | 0.46 | 99.9 |
| | 7 | 99.44 | 99.72 | 99.18 | 99.72 | 99.45 | 0.28 | 0.82 | 100 |
| | 10 | 99.63 | 99.59 | 99.68 | 99.58 | 99.64 | 0.42 | 0.32 | 99.9 |
| FCM-DNN | 5 | 99.66 | 100 | 99.31 | 100 | 99.65 | 0 | 0.69 | 100 |
| | 7 | 99.70 | 99.86 | 99.54 | 99.86 | 99.7 | 0.14 | 0.46 | 100 |
| | **10** | **99.91** | **100** | **99.82** | **100** | **99.91** | **0** | **0.18** | **100** |

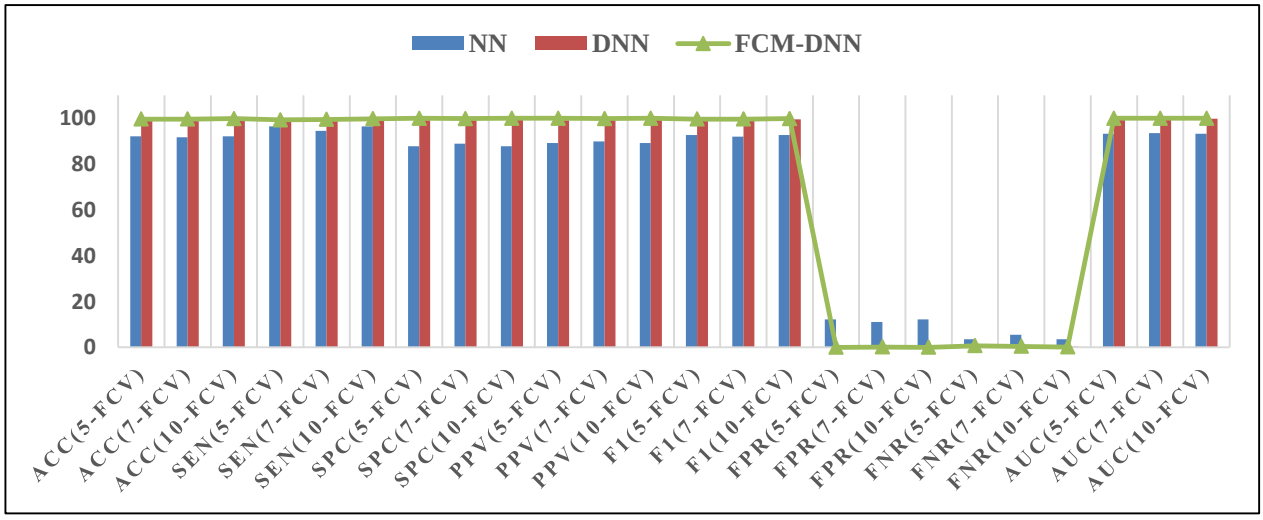


**Figure 13.** A Comparison between NN, DNN, and FCM-DNN methods.

According to Figure 13, the better performance of the FCM-DNN method compared to the NN and DNN methods is observed in terms of the evaluation criteria. Therefore, diagnosis and decision-making regarding the CAD are guaranteed using the FCM-DNN method.

As a final result, based on related works in table 5, for the first time, in this paper, NN, DNN, and FCM-DNN methods were presented on the CMRI dataset. The FCM-DNN method has the best accuracy of 99.91% on 4965 images.

**Table 5.** CAD diagnosis using artificial intelligence methods.

| Authors | ACC (%) | Methods | The dataset |
|---|---|---|---|
| Verma et al., [42] | 88.4 | MLR | 335 samples |
| Arabasadi et al., [31] | 93.85 | NN-GA (10-FCV) | 303 samples |
| Alizadehsani et al., [32] | 96.4 | SVM (10-FCV) | 500 samples |
| Miaoa and Miaoa., [34] | 83.67 | DNN | 303 samples |
| Abdar et al., [33] | 93.08 | N2Genetic-NuSVM (10-FCV) | 303 samples |
| Hassannataj et al. [17] | 91.47 | RTs(10-FCV) | 303 samples |
| Ghiasi et al. [41] | 100 | CART | 303 samples |
| Idris et al. [43] | 94.5% | NN with embedded decision tree features | 5100 samples |
| Velusamy and Ramasamy, [44] | 98.97 | weighted-average voting | 303 samples |
| Acharia et al. [39] | 98.5 | KNN (10-FCV) | 52091 ECG signals |
| Tan et al. [38] | 99.85 | LSTM-CNN | 38120 ECG signals |
| Hamersvelt et al., [35] | 98.5 | CNN | Angiography CT images with 126 patients |
| Acharya et al. [40] | 98.97 | CNN (10-FCV) | 140000 ECG signals |
| In this paper | 99.91 | FCM-DNN | 4965 CMRI |

## 4. Conclusion and Future Works

Coronary artery disease is known as coronary artery stenosis, which is the most common disease in middle-aged and older people. Heart disease [65] is occurred by the accumulation of platelets in the arteries. Following this event, blood flow is clogged leading to heart failure. The most popular tool for diagnosing CAD disease is angiography, which has side effects [66].

In recent years, many studies have been conducted to develop artificial intelligence-based methods instead of angiography. Hence, in this paper, NN, DNN, and FCM-DNN methods were applied for CAD diagnosis on the CMRI dataset. The results illustrate that the proposed FCM-DNN method has the best accuracy rate of 99.91%, and also the FCM-DNN method has the least false rate compared to the NN and DNN methods, which the results were dedicated in Table 4. As an important result, no studies have been run for CAD diagnosis on the CMRI dataset so far, as shown in Table 5.

For future work, The FCM-DNN method can be used as a computer-aided diagnosis system for CAD diagnosis in clinical centers. In addition, we suggest that a combination of evolutionary and deep learning methods be developed for CAD diagnosis on the CMRI dataset, and also a deep convolutional neural network in combination with evolutionary methods can be investigated.

## References


1. Jiang F, Jiang Y, Zhi H, et al. (2017) Artificial intelligence in healthcare: past, present and future. *Stroke and vascular neurology* 2.
2. McCradden MD, Stephenson EA, Anderson JA (2020) Clinical research underlies ethical integration of healthcare artificial intelligence. *Nature Medicine* 26: 1325-1326.
3. Yu K-H, Beam AL, Kohane IS (2018) Artificial intelligence in healthcare. *Nature biomedical engineering* 2: 719-731.
4. Asan O, Bayrak AE, Choudhury A (2020) Artificial intelligence and human trust in healthcare: focus on clinicians. *Journal of medical Internet research* 22: e15154.
5. Shen D, Wu G, Suk H-I (2017) Deep learning in medical image analysis. *Annual review of biomedical engineering* 19: 221-248.
6. Litjens G, Kooi T, Bejnordi BE, et al. (2017) A survey on deep learning in medical image analysis. *Medical image analysis* 42: 60-88.
7. Razzak MI, Naz S, Zaib A (2018) Deep learning for medical image processing: Overview, challenges and the future. *Classification in BioApps*: 323-350.
8. Thrall JH, Fessell D, Pandharipande PV (2021) Rethinking the approach to artificial intelligence for medical image analysis: the case for precision diagnosis. *Journal of the American College of Radiology* 18: 174-179.
9. Zhang Y, Wang Z, Zhang J, et al. (2021) Deep learning model for classifying endometrial lesions. *Journal of Translational Medicine* 19: 1-13.
10. Zheng C, Chen L, Jian J, et al. Efficacy evaluation of interventional therapy for primary liver cancer using magnetic resonance imaging and CT scanning under deep learning and treatment of vasovagal reflex. *The Journal of Supercomputing*: 1-14.
11. Roth GA, Johnson C, Abajobir A, et al. (2017) Global, regional, and national burden of cardiovascular diseases for 10 causes, 1990 to 2015. *Journal of the American College of Cardiology* 70: 1-25.
12. Miao KH, Miao JH (2018) Coronary heart disease diagnosis using deep neural networks. *Int J Adv Comput Sci Appl* 9: 1-8.
13. Gupta A, Arora HS, Kumar R, et al. DMHZ: A Decision Support System Based on Machine Computational Design for Heart Disease Diagnosis Using Z-Alizadeh Sani Dataset; 2021. IEEE. pp. 818-823.
14. Villa AD, Sammut E, Nair A, et al. (2016) Coronary artery anomalies overview: the normal and the abnormal. *World journal of radiology* 8: 537.
15. Alizadehsani R, Abdar M, Roshanzamir M, et al. (2019) Machine learning-based coronary artery disease diagnosis: A comprehensive review. *Computers in biology and medicine* 111: 103346.
16. Williamson TM, Moran C, McLennan A, et al. (2020) Promoting adherence to physical activity among individuals with cardiovascular disease using behavioral counseling: A theory and research-based primer for health care professionals. *Progress in Cardiovascular Diseases*.
17. Joloudari JH, Hassannataj Joloudari E, Saadatfar H, et al. (2020) Coronary artery disease diagnosis; ranking the significant features using a random trees model. *International journal of environmental research and public health* 17: 731.
18. Van Dyke M, Greer S, Odom E, et al. (2018) Heart disease death rates among blacks and whites aged≥ 35 years—United States, 1968–2015. *MMWR Surveillance Summaries* 67: 1.

19. Mozaffarian D, Benjamin EJ, Go AS, et al. (2015) Heart disease and stroke statistics—2015 update: a report from the American Heart Association. *circulation* 131: e29-e322.
20. Benjamin EJ, Virani SS, Callaway CW, et al. (2018) Heart disease and stroke statistics—2018 update: a report from the American Heart Association. *Circulation*.
21. Larochelle H, Bengio Y, Louradour J, et al. (2009) Exploring strategies for training deep neural networks. *Journal of machine learning research* 10.
22. Bonow RO, Mann DL, Zipes DP, et al. (2011) Braunwald's heart disease e-book: A textbook of cardiovascular medicine: Elsevier Health Sciences.
23. Nabel EG, Braunwald E (2012) A tale of coronary artery disease and myocardial infarction. *New England Journal of Medicine* 366: 54-63.
24. Babaoglu İ, Findik O, Ülker E (2010) A comparison of feature selection models utilizing binary particle swarm optimization and genetic algorithm in determining coronary artery disease using support vector machine. *Expert Systems with Applications* 37: 3177-3183.
25. Kumar M, Pachori RB, Acharya UR (2017) Characterization of coronary artery disease using flexible analytic wavelet transform applied on ECG signals. *Biomedical signal processing and control* 31: 301-308.
26. Alizadehsani R, Habibi J, Hosseini MJ, et al. (2012) Diagnosis of coronary artery disease using data mining techniques based on symptoms and ecg features. *European Journal of Scientific Research* 82: 542-553.
27. Alizadehsani R, Habibi J, Hosseini MJ, et al. (2013) A data mining approach for diagnosis of coronary artery disease. *Computer methods and programs in biomedicine* 111: 52-61.
28. Alizadehsani R, Habibi J, Sani ZA, et al. (2013) Diagnosing coronary artery disease via data mining algorithms by considering laboratory and echocardiography features. *Research in cardiovascular medicine* 2: 133.
29. Alizadehsani R, Zangooei MH, Hosseini MJ, et al. (2016) Coronary artery disease detection using computational intelligence methods. *Knowledge-Based Systems* 109: 187-197.
30. Dolatabadi AD, Khadem SEZ, Asl BM (2017) Automated diagnosis of coronary artery disease (CAD) patients using optimized SVM. *Computer methods and programs in biomedicine* 138: 117-126.
31. Arabasadi Z, Alizadehsani R, Roshanzamir M, et al. (2017) Computer aided decision making for heart disease detection using hybrid neural network-Genetic algorithm. *Computer methods and programs in biomedicine* 141: 19-26.
32. Alizadehsani R, Hosseini MJ, Khosravi A, et al. (2018) Non-invasive detection of coronary artery disease in high-risk patients based on the stenosis prediction of separate coronary arteries. *Computer methods and programs in biomedicine* 162: 119-127.
33. Abdar M, Książek W, Acharya UR, et al. (2019) A new machine learning technique for an accurate diagnosis of coronary artery disease. *Computer methods and programs in biomedicine* 179: 104992.
34. Newman DJ, Hettich S, Blake CL, et al. (1998) UCI repository of machine learning databases, 1998.
35. van Hamersvelt RW, Zreik M, Voskuil M, et al. (2019) Deep learning analysis of left ventricular myocardium in CT angiographic intermediate-degree coronary stenosis improves the diagnostic accuracy for identification of functionally significant stenosis. *European radiology* 29: 2350-2359.
36. Acharya UR, Fujita H, Lih OS, et al. (2017) Automated detection of coronary artery disease using different durations of ECG segments with convolutional neural network. *Knowledge-Based*

*Systems* 132: 62-71.
37. Goldberger AL, Amaral LA, Glass L, et al. (2000) PhysioBank, PhysioToolkit, and PhysioNet: components of a new research resource for complex physiologic signals. *circulation* 101: e215-e220.
38. Tan JH, Hagiwara Y, Pang W, et al. (2018) Application of stacked convolutional and long short-term memory network for accurate identification of CAD ECG signals. *Computers in biology and medicine* 94: 19-26.
39. Acharya UR, Fujita H, Adam M, et al. (2017) Automated characterization and classification of coronary artery disease and myocardial infarction by decomposition of ECG signals: A comparative study. *Information Sciences* 377: 17-29.
40. Acharya UR, Fujita H, Oh SL, et al. (2019) Deep convolutional neural network for the automated diagnosis of congestive heart failure using ECG signals. *Applied Intelligence* 49: 16-27.
41. Ghiasi MM, Zendehboudi S, Mohsenipour AA (2020) Decision tree-based diagnosis of coronary artery disease: CART model. *Computer Methods and Programs in Biomedicine* 192: 105400.
42. Verma L, Srivastava S, Negi P (2016) A hybrid data mining model to predict coronary artery disease cases using non-invasive clinical data. *Journal of medical systems* 40: 178.
43. Idris NM, Chiam YK, Varathan KD, et al. (2020) Feature selection and risk prediction for patients with coronary artery disease using data mining. *Medical & biological engineering & computing* 58: 3123-3140.
44. Velusamy D, Ramasamy K (2020) Ensemble of heterogeneous classifiers for diagnosis and prediction of coronary artery disease with reduced feature subset. *Computer Methods and Programs in Biomedicine* 198: 105770.
45. Goodfellow I, Warde-Farley D, Mirza M, et al. Maxout networks; 2013. PMLR. pp. 1319-1327.
46. Joloudari JH, Haderbadi M, Mashmool A, et al. (2020) Early detection of the advanced persistent threat attack using performance analysis of deep learning. *IEEE Access* 8: 186125-186137.
47. Ito Y (1991) Approximation of functions on a compact set by finite sums of a sigmoid function without scaling. *Neural Networks* 4: 817-826.
48. Hassan1, 2 N, Akamatsu N (2004) A new approach for contrast enhancement using sigmoid function.
49. Li X, Zhang X, Huang W, et al. (2020) Truncation Cross Entropy Loss for Remote Sensing Image Captioning. *IEEE Transactions on Geoscience and Remote Sensing*.
50. Otto C, Wang D, Jain AK (2017) Clustering millions of faces by identity. *IEEE transactions on pattern analysis and machine intelligence* 40: 289-303.
51. Ruspini EH (1969) A new approach to clustering. *Information and control* 15: 22-32.
52. Duda RO, Hart PE Pattern classification and scene analysis.
53. Veloso R, Portela F, Santos MF, et al. (2014) A clustering approach for predicting readmissions in intensive medicine. *Procedia Technology* 16: 1307-1316.
54. Park H-S, Jun C-H (2009) A simple and fast algorithm for K-medoids clustering. *Expert systems with applications* 36: 3336-3341.
55. Duda RO, Hart PE (1973) Pattern classification and scene analysis: Wiley New York.
56. Dunn JC (1974) Well-separated clusters and optimal fuzzy partitions. *Journal of cybernetics* 4: 95-104.
57. Bezdek JC (1981) Objective function clustering. *Pattern recognition with fuzzy objective function algorithms*: Springer. pp. 43-93.

58. Yang M-S (1993) A survey of fuzzy clustering. *Mathematical and Computer modelling* 18: 1-16.
59. Govaert G, Nadif M (2003) Clustering with block mixture models. *Pattern Recognition* 36: 463-473.
60. Bandyopadhyay S, Maulik U, Mukhopadhyay A (2007) Multiobjective genetic clustering for pixel classification in remote sensing imagery. *IEEE transactions on Geoscience and Remote Sensing* 45: 1506-1511.
61. Xu R, Wunsch D (2005) Survey of clustering algorithms. *IEEE Transactions on neural networks* 16: 645-678.
62. Joloudari JH, Saadatfar H, Dehzangi A, et al. (2019) Computer-aided decision-making for predicting liver disease using PSO-based optimized SVM with feature selection. *Informatics in medicine unlocked* 17: 100255.
63. Abdar M, Zomorodi-Moghadam M, Das R, et al. (2017) Performance analysis of classification algorithms on early detection of liver disease. *Expert Systems with Applications* 67: 239-251.
64. Weng C-H, Huang TC-K, Han R-P (2016) Disease prediction with different types of neural network classifiers. *Telematics and Informatics* 33: 277-292.
65. Diwakar M, Tripathi A, Joshi K, et al. (2021) Latest trends on heart disease prediction using machine learning and image fusion. *Materials Today: Proceedings* 37: 3213-3218.
66. Moon JH, Cha WC, Chung MJ, et al. (2021) Automatic stenosis recognition from coronary angiography using convolutional neural networks. *Computer methods and programs in biomedicine* 198: 105819.